Large Deflection of Shallow Rectangular Shell Panels

ROBERT R. ARCHER* AND PEI-KAO HSUEH†
University of Massachusetts, Amherst, Mass.

Nonsymmetric deflections of shallow shell panels are studied in the nonlinear range. Snap-through buckling loads for spherical panels on a square base are computed for a wide range of shell geometries by a direct solution of appropriate nonlinear finite difference equations. This work extends previously known results for spherical shells on a circular base. Details are given as to the application of the procedures developed to different load and support conditions for given shallow shell geometries.

Nomenclature

A	=	reference x dimension for rectangular base
A_{ij}	=	matrices used in iteration
B	=	reference y dimension for rectangular base
D	=	Eh^3/m^4 = flexural stiffness for shell
E	=	Young's modulus
F	=	$\nabla^2 w$
h	=	thickness of shell
H	=	moment stress resultant
H_0	=	central height of shallow shell
h_x,h_y	=	grid increments in x and y directions
$k_x,k_y,\bar{k}$	=	nondimensional curvature expressions
K_x,K_y	=	curvatures of the shell
K_x	=	$(A^2/h)\,(-3K_x - K_y)$, $K_y = (A^2/h)\,(-3K_y - K_x)$
$\bar{K}$	=	$(6A^4/h^2)\,(K_x + \frac{2}{3}K_xK_y + K_y^2)$
m^2	=	$[12(1-\mu^2)]^{1/2}$
M	=	number of internal grid points—y direction
M_x,M_y	=	moment stress resultants
N	=	number of internal grid points—x direction
p,p_{cr}	=	nondimensional pressure, snap pressure
$q,\tilde{q}$	=	transverse pressure, nondimensional pressure, $q = [Eh^4/6(1-\mu^2)A^4]\tilde{q}$
q_{cr}	=	classical buckling pressure complete sphere
Q_x,Q_y	=	shear force resultants
R	=	radius of spherical shell
S_x,S_y,S_{xy}	=	nondimensional stress resultants
u,v,w	=	nondimensional displacements
U,V,W	=	tangential and normal displacements
$u_i{}^j,v_i{}^j,w_i{}^j,F_i{}^j$	=	grid values of unknowns
$\mathbf{u},\mathbf{v},\mathbf{w},\mathbf{F}$	=	column vectors of grid points
$\Delta\mathbf{u},\Delta\mathbf{v},\Delta\mathbf{w},\Delta\mathbf{F}$	=	corrections to grid vectors
w_{av}	=	average value of $w_i{}^j$ over grid
x,y	=	nondimensional coordinates, $x = X/A$, $y = Y/A$
X,Y	=	middle surface coordinates
β	=	$A^2m^4/4R^2$
$\epsilon_x,\epsilon_y,\gamma$	=	middle surface strains
λ	=	$mA/(4hR)^{1/2}$
μ	=	Poisson's ratio (take $\mu = \frac{1}{3}$)
ρ	=	mass density of shell
σ_x,σ_y,τ	=	membrane stresses
δ_x,δ_y	=	central difference operators
∇^2	=	$\partial^2/\partial x^2 + \partial^2/\partial y^2$ or $\partial^2/\partial X^2 + \partial^2/\partial Y^2$

1. Introduction

IT is well known that certain types of buckling phenomenon connected with thin plate and shell elements are only revealed by employing a nonlinear large deflection analysis. Because of the complexity of these problems, it has only been in recent years that accurate solution methods have been available for this analysis.

In the present work a particular class of shells is studied by means of a finite difference iteration method. Shallow shell panels on a rectangular base represent practically important structural components for which little is known about their buckling characteristics under transverse loads except for a few examples where assumed mode type approximate solutions have been obtained.[1]

The particular case of a square spherical shell panel under uniform and point transverse loads is of particular interest since it should be fairly similar in its behavior to the corresponding spherical shell panel on a circular base. The later problem has been extensively studied and both symmetric snap-through loads as well as nonsymmetric bifurcation buckling loads have been found. (For uniform transverse pressure see Ref. 2 and for point loads at the apex see Ref. 3.) However, once the technique for the study of this class of nonsymmetric problems is developed, it can be applied to a wide class of load systems and combinations of edge support conditions.

2. Basic Equations

Equations describing the nonlinear deflection of shallow shells are given in the Appendix. The governing equations can be found in Ref. 1 and take the following form ($\mu = \frac{1}{3}$):

$$3u_{xx} + u_{yy} + 2v_{xy} + w_x(k_x + 3w_{xx} + w_{yy}) + 2w_{xy}w_y = G_1 = 0 \quad (1)$$

$$3v_{yy} + v_{xx} + 2u_{xy} + w_y(k_y + 3w_{yy} + w_{xx}) + 2w_{xy}w_x = G_2 = 0 \quad (2)$$

$$\tfrac{1}{2}\nabla^2 F + 2k_xu_x + 2k_yv_y + \bar{k}w + k_xw_x^2 + k_yw_y^2 - S_xw_{xx} - S_yw_{yy} - S_{xy}w_{xy} - \tilde{q} = G_3 = 0 \quad (3)$$

$$\nabla^2 w - F = G_4 = 0 \quad (4)$$

In each case Eqs. (1–4) must be solved for particular boundary conditions.

3. Method of Analysis

The solution procedure consists of writing Eqs. (1–4) in finite difference form. (See Figs. 1 and 2). The resulting simultaneous nonlinear algebraic equations are solved by a Newton Raphson iteration.[5]

In the Appendix it is shown that at each stage of the iteration leading to a solution of these equations it is necessary to solve the following $(4M \times N) \times (4M \times N)$ system of linear

Received November 12, 1968; revision received April 28, 1969. The work of both authors was sponsored in part by Grant GK-1856 from the National Science Foundation.

* Professor of Civil Engineering.
† Graduate Assistant. Member AIAA.

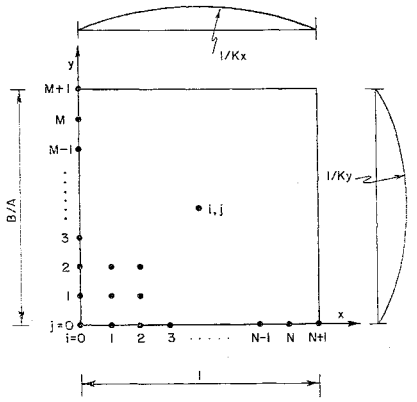

Fig. 1 Grid of solution points on rectangular panel.

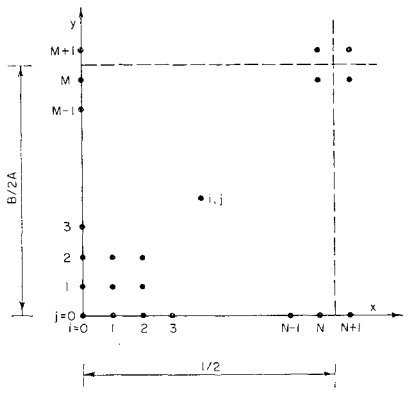

Fig. 2 Quarter panel for symmetric case.

equations:

$$\begin{pmatrix} A_{11} & A_{12} & A_{13} & 0 \\ A_{21} & A_{22} & A_{23} & 0 \\ A_{31} & A_{32} & A_{33} & A_{34} \\ 0 & 0 & A_{43} & A_{44} \end{pmatrix} \begin{pmatrix} \Delta\mathbf{u} \\ \Delta\mathbf{v} \\ \Delta\mathbf{w} \\ \Delta\mathbf{F} \end{pmatrix} = \begin{pmatrix} A_{15} \\ A_{25} \\ A_{35} \\ 0 \end{pmatrix} \tag{5}$$

where N and M are the number of internal grid points in the x and y directions, and the $\Delta\mathbf{u}$, $\Delta\mathbf{v}$, $\Delta\mathbf{w}$, $\Delta\mathbf{F}$ are vectors which give the "corrections" at each stage to the previously estimated solution of the original nonlinear finite difference equations.

Since the equations are nonlinear, the A_{ij}'s are defined in terms of the most recent estimate of the solution vectors, say

$$\mathbf{u}_0,\mathbf{v}_0,\mathbf{w}_0,\mathbf{F}_0 \tag{6}$$

After each cycle of the iteration we have

$$\mathbf{u} = \mathbf{u}_0 + \Delta\mathbf{u} \tag{7}$$

$$\mathbf{v} = \mathbf{v}_0 + \Delta\mathbf{v} \tag{8}$$

$$\mathbf{w} = \mathbf{w}_0 + \Delta\mathbf{w} \tag{9}$$

$$\mathbf{F} = \mathbf{F}_0 + \Delta\mathbf{F} \tag{10}$$

as the most recent estimate of the solution.

It may be noted that A_{34}, A_{43}, and A_{44} are constant matrices for given boundary conditions, and thus the system can be reduced to a 3×3 form for the iteration. Also since A_{11}, A_{12}, A_{21}, and A_{22} are constant matrices, the inverse of that part of the whole matrix need only be computed once. This is due to the fact that (1) and (2) involve u and v in a linear fashion.

Each of the matrices A_{ij} consist of tridiagonal "banded" submatrices each of which are themselves banded about the diagonal. For example, for a simply supported shell,

$$A_{11} = \begin{bmatrix} P_1 & P_2 & & 0 \\ P_2 & P_1 & & \\ & & \ddots & P_2 \\ 0 & & P_2 & P_1 \end{bmatrix}$$

and

$$P_1 = \begin{bmatrix} a & 3/h_x^2 & & \\ & \ddots & \ddots & 0 \\ 3/h_x^2 & & \ddots & 3/h_x^2 \\ & \ddots & & \\ 0 & & 3/h_x^2 & a \end{bmatrix}$$

$$P_2 = (1/h_y^2)\mathrm{I}$$

where I is the $N \times N$ identity matrix.

Although some advantage could be taken of the form of these matrices by writing special elimination and matrix handling schemes, experience with closely related problems indicates that the additional logical operations end up taking enough time so that the extra programing effort is not warranted.

For axisymmetric problems[4] where the whole system is tridiagonal (banded), the use of algorithms which solve the system by elimination of the "below" diagonal terms to get an upper triangular matrix is very fast and efficient.

The analysis of a given shell panel proceeds as follows: 1) starting from a known deflection state (usually zero load/no deflection) an independent load or deflection parameter is incremented; 2) the iteration is attempted; if it converges further increments are taken, if not then smaller increments are attempted. By this procedure it is possible to obtain a sequence of equilibrium states revealing the static behavior of the shell in the nonlinear large deflection range of loading.

4. Discussion of Results

The first examples that were studied were shallow spherical shells for both simply supported and fixed conditions at the edges of a square supporting frame.

If a nondimensional uniform pressure is defined by

$$p = q/q_{cr} \tag{11}$$

where

$$q_{cr} = 4Eh^2/R^2m^2 \tag{12}$$

Table 1 Deflection modes along the half diagonal at intermediate load and snap load (spherical shell on square base); 12 × 12, λ = 4.0

		w(at $I = J$)					
Edge condition	P	1	2	3	4	5	6
Simply supported	0.4	0.04142	0.12647	0.20569	0.25584	0.27785	0.28392
	0.7	0.09026	0.29806	0.49765	0.58818	0.57108	0.52754
Clamped edges	0.4	0.01187	0.06238	0.14447	0.23416	0.30761	0.34826
	0.575	0.01468	0.08250	0.21278	0.38759	0.56142	0.67186

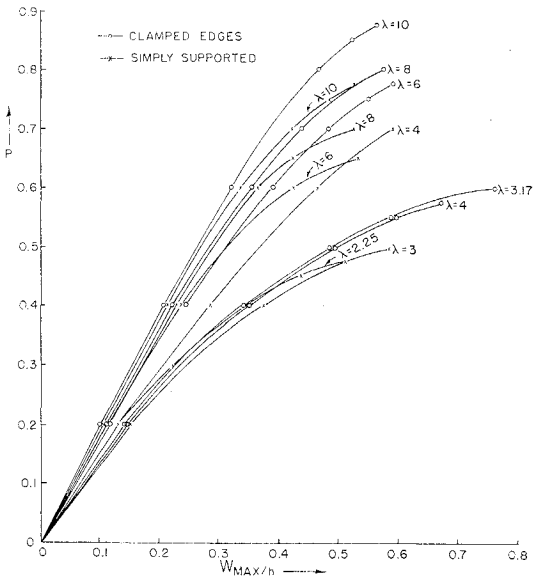

Fig. 3 Load deflection curves (12 × 12 grid).

is the classical buckling pressure of a complete spherical shell of radius R and thickness h, then it is convenient to define the geometric parameter

$$\lambda^2 = (m^2/4)(A^2/hR) \tag{13}$$

With these parameters it is possible to make direct comparisons with the corresponding inscribed spherical cap of radius R and base diameter of A. For inward directed pressures, the axisymmetric snap-through loads have been calculated by Weinitschke[6] and others. In Fig. 3 are shown the load-maximum deflection curves for various λ values using a 12 × 12 grid of internal points (i.e., $M = N = 6$ for the symmetric case).

These curves were found by stepping the pressure p and halting the computation when Δp increments of less than 0.02 resulted in no convergence. These represent lower bounds on the snap-through loads for the square panels.

Experiences with independent calculations using w_{AV} (the average value of $w_i{}^j$ over the square) indicate that the peak pressures shown in Fig. 3 are very near the actual snap pressures for a given shell with a fixed grid refinement.

In Figs. 4 and 5 and Table 1, the deflection modes for the various shells just at the onset of snap buckling are given. It is seen that as λ increases (i.e., the ratio $H_0/h = \lambda^2/m^2$ where H_0 is the central height of the spherical panel) the panels shows increasing waviness. As expected, it is necessary to include more points in the grid to achieve more accuracy in the estimation of the buckling load. In Fig. 6 and Table 2, the influence of the grid refinement is seen. As more effective degrees of freedom are added, the snapping

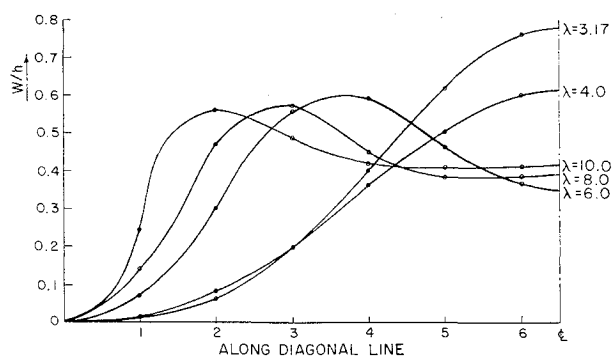

Fig. 4 Deflection modes at onset of snap buckling (12 × 12 grid) with fixed edges.

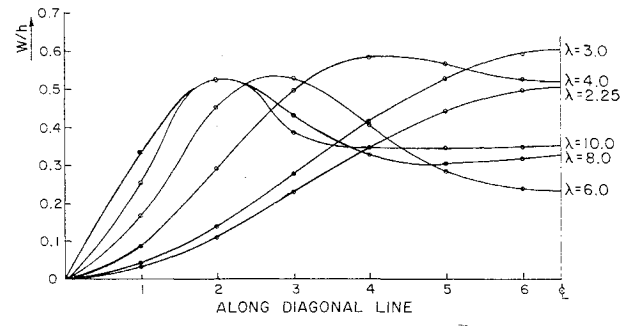

Fig. 5 Deflection modes at onset of snap buckling (12 × 12 grid) with simply supported edges.

occurs at lower values. The spread of the correction is dependent on the complexity of the buckling mode shape.

The 12 × 12 grid was the largest size convenient for a 32K computer memory without the use of backup storage. The computer program automatically constructed all the matrices for an arbitrary grid so that with backup memory use much larger grids could be used, but with the correspondingly slower times.

The results for symmetric snap-through loads p_{cr} are shown in Fig. 7 for the 12 × 12 grid. The general trend of minimum values for λ for the initiation of buckling and the shape of the $p_{cr} - \lambda$ curve for small λ is similar. However, although the fixed edge circular cap between $\lambda^2 = 30$ and 85 rises above $p_{cr} = 1$ the square cap remains very flat with λ. Perhaps the geometry of the square cap permits added flexibility due to the corners. It should be noted that the results of Fig. 6 are a warning that the values shown in Fig. 7 become increasingly less reliable with increasing λ.

In Ref. 2, Huang found that nonsymmetric buckling can be initiated for circular panels at loads less than the snap-through loads. This initiation of nonsymmetric buckling before snap buckling was also studied here for the square panel. This buckling possibly would be signaled by a change in sign of the determinant of the left side in (5) for a given load and deflection state. We did find bifurcation buckling for cases with $\lambda \geq 6$ but they occurred very near to the snap loads. They had very little practical significance. Also since for the full nonsymmetric case we were only able to use a 6 × 6 grid, it is seen from Fig. 6 that for $\lambda \geq 6$ the 6 × 6 results may be 50% too high. Thus the investigation of the possibility of bifurcation from the symmetric states before snap buckling occurs remains to be investigated.

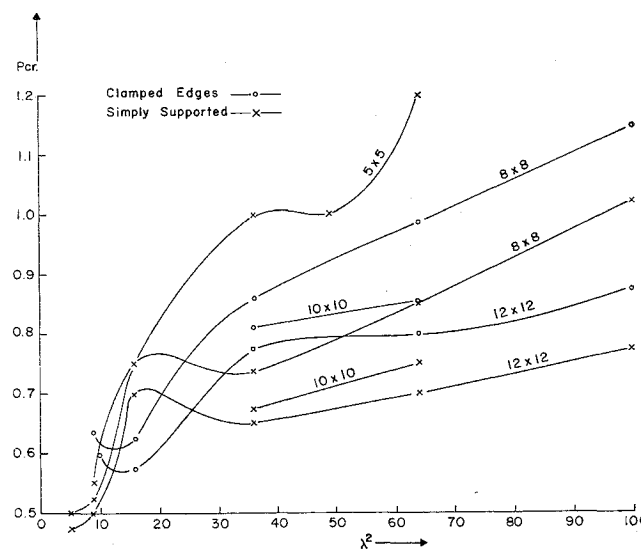

Fig. 6 Snap buckling loads for different grid sizes.

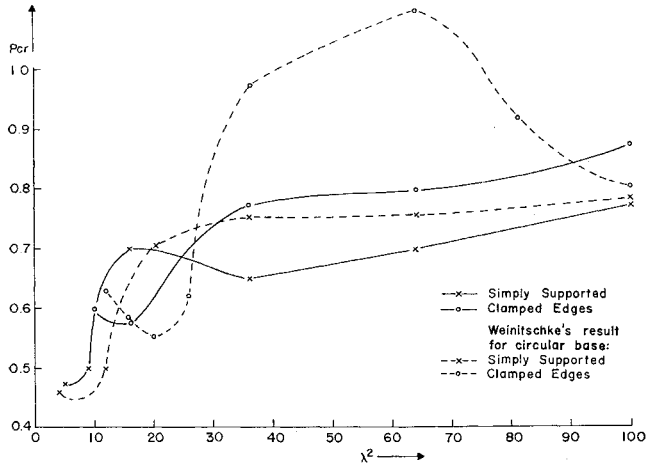

Fig. 7 Comparison of snap buckling loads for square panel and circular cap.[6]

In order to investigate states for deflections beyond the last points shown in Fig. 3, it is convenient to introduce another independent parameter

$$w_{av} = \frac{1}{MN} \sum_{i=1}^{N} \sum_{j=1}^{M} w_i{}^j \tag{14}$$

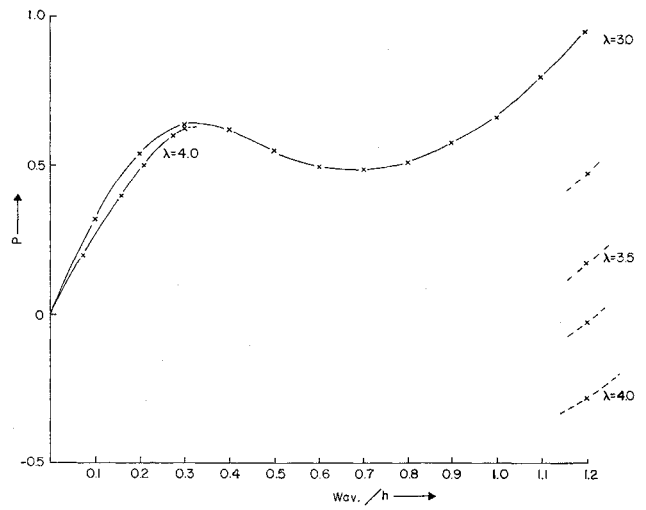

Fig. 8 Points on postbuckling curves for square panel with fixed edges (8 × 8 grid).

and consider w_{av} as prescribed and p as a variable (see A-3). With this approach the pressure decreases for deflection points beyond the last points shown in Fig. 3. In particular, Fig. 8 shows the postbuckling curve for $\lambda = 3$ and Figs. 9 and 10 give deflection modes. Once a postbuckling curve is obtained it is possible to get postbuckling curves for other values of λ by holding the w_{av} fixed and changing the λ values. Such results are given in Fig. 8. The results shown in Fig. 8 for $\lambda > 3$ would be expected to follow the same general trend as shown for $\lambda = 3$, but considerable care must be taken for larger values of λ, since it can happen that a shift to another "branch" of the nonlinear equilibrium curves can occur.

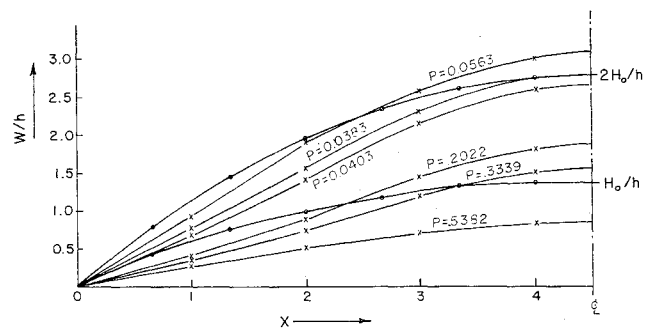

Fig. 9 Deflection modes compared with initial rise parabola of shell and reversed parabola ($\lambda = 3$ simply supported, 8 × 8 grid).

Table 2 Snap buckling loads and maximum deflections for various grid sizes (spherical shell on square base)[a]

Edge condition	λ	P_{cr} 5×5	8×8	10×10	12×12	W_{MAX} (12×12)
Simply supported	2.25		0.500		0.475	0.50466
	3.0	0.550	0.525		0.500	0.59563
	4.0	0.750	0.750		0.700	0.58818
	6.0	1.000	0.738	0.675	0.650	0.53156
	8.0	1.200	0.850	0.750	0.700	0.52412
	10.0	1.800	1.025		0.775	0.52503
Clamped edges	3.17				0.600	0.75555
	4.0		0.625		0.575	0.67186
	6.0		0.863	0.813	0.775	0.58888
	8.0		0.988	0.850	0.800	0.57250
	10.0		1.150		0.875	0.56287

[a] Additional calculations carried out in a related study show that for $\lambda = 5$ and a 12 × 12 grid, P_{cr} and W_{MAX} for the simply supported case were 0.650 and 0.50390, and for the clamped case 0.850 and 0.71537, respectively. Thus the curve for the 12 × 12 grid in Figs. 6 and 7 would be modified accordingly between $\lambda^2 = 20$ and 30.

The computer programs developed for this analysis are general in the sense that for fixed or simply supported rectangular shell panels with k_x and k_y given, symmetric or nonsymmetric loading, the iteration matrices are automatically set up for arbitrary grid variables M and N.

For example, a simply supported rectangular spherical shell panel with $\lambda = 4$, $B = 2A$, $M = 12$, $N = 6$ subjected to a uniform pressure was considered and the snap buckling load found to be $p_{cr} = 0.59$. This is to be compared with a corresponding square panel with $\lambda = 4$, $B = A$, $M = 12$, $N = 12$ when $p_{cr} = 0.70$. See Table 3 for other results. A cylindrical panel was also considered and the results are shown in Table 4. Although the preceding examples were restricted to fixed and simply supported boundary conditions, it is clear that the method could be easily applied to other combinations of edge conditions.

5. Conclusions

1) Symmetric and nonsymmetric nonlinear deflection states for shallow rectangular shell panels can be efficiently computed by a Newton-type iteration of the finite difference equations.

2) The predicted snap-through buckling loads for transversely loaded spherical shell panels on a rectangular base follow the general trend of the corresponding known results for a spherical panel on a circular base.

3) Other cases of shell geometry, load, and support conditions where deflection states in the nonlinear range are required may be studied by these methods.

Table 3 Snap buckling loads and maximum deflections (spherical shell on $A \times 2A$ rectangular base); $B = 2A$, 6×12, $\lambda = 4.0$, $K_x = K_y = 1/R$

Edge condition	P_{cr}	W_{MAX}
Simply supported	0.5916	0.40839
Clamped edges	0.6544	0.49265

Table 4 Snap buckling loads and maximum deflections (cylindrical shell on $A \times 2A$ rectangular base); $B = 2A$, 6×12, $k_y = 0$

Edge condition	λ	P_{cr}	W_{MAX}
Simply supported	3.0	0.1750	0.43469
	4.0	0.2460	0.63994
	6.0	0.2750	0.51371
Clamped edges	3.0	0.2250	0.46508
	4.0	0.2244	0.60476
	6.0	0.2500	0.53563

Appendix

A-1. Finite Difference Form of the Shell Equations

If each derivative in (1–4) is replaced by the appropriate central difference expression we obtain

$$3\frac{\delta_x^2 u_i^j}{h_x^2} + \frac{\delta_y^2 u_i^j}{h_y^2} + 2\frac{\delta_x\delta_y}{4h_xh_y}v_i^j + \frac{\delta_x w_i^j}{2h_x}\left(k_x + 3\frac{\delta_x^2}{h_x^2}w_i^j + \frac{\delta_y^2}{h_y^2}w_i^j\right) + 2\frac{\delta_x\delta_y}{4h_xh_y}w_i^j\frac{\delta_y}{2h_y}w_i^j = \tilde{G}_1 = 0 \quad \text{(A1)}$$

$$3\frac{\delta_y^2}{h_y^2}v_i^j + \frac{\delta_x^2}{h_x^2}v_i^j + 2\frac{\delta_x\delta_y}{4h_xh_y}u_i^j + \frac{\delta_y w_i^j}{2h_y}w_i^j \times \left(k_y + 3\frac{\delta_y^2}{h_y^2}w_i^j + \frac{\delta_x^2}{h_x^2}w_i^j\right) + 2\frac{\delta_x\delta_y}{4h_xh_y}w_i^j\frac{\delta_x}{2h_x}w_i^j = \tilde{G}_2 = 0 \quad \text{(A2)}$$

$$\frac{1}{2}\left(\frac{\delta_x^2}{h_x^2} + \frac{\delta_y^2}{h_y^2}\right)F_i^j + 2k_x\frac{\delta_x}{2h_x}u_i^j + 2k_y\frac{\delta_y}{2h_y}v_i^j + \bar{K}w_i^j + k_x\left(\frac{\delta_x}{2h_x}w_i^j\right)^2 + k_y\left(\frac{\delta_y}{2h_y}w_i^j\right)^2 - S_{x_i}{}^j\frac{\delta_x^2}{h_x^2}w_i^j - S_{y_i}{}^j\frac{\delta_y^2}{h_y^2}w_i^j - S_{xy_i}{}^j\frac{\delta_x\delta_y}{4h_xh_y}w_i^j - \tilde{q}_i^j = \tilde{G}_3 = 0 \quad \text{(A3)}$$

$$\left(\frac{\delta_x^2}{h_x^2} + \frac{\delta_y^2}{h_y^2}\right)w_i^j - F_i^j = \tilde{G}_4 = 0 \quad \text{(A4)}$$

where

$$h_x = 1/(N+1),\ h_y = (B/A)/(M+1) \quad \text{(A5,6)}$$

and δ_x and δ_y are central difference operators with respect to the spacings h_x and h_y.

A-2. Matrices for Newton-Raphson Method

If we order the two-dimensional array of internal points by rows (i.e., along the x direction), then $M \times N$ dimensional vectors $\mathbf{u}$, $\mathbf{v}$, $\mathbf{w}$, $\mathbf{F}$ are defined by the solution values at these points.

In accordance with the Newton iteration we can derive a set of linear equations for the corrections to a previous set of estimates, say $\Delta\mathbf{u}$, $\Delta\mathbf{v}$, $\Delta\mathbf{w}$, $\Delta\mathbf{F}$. If we write Eq. (A1) at each point (row by row) followed by (A2, A3, and A4) at each point, then we have a $(4M \times N) \times (4M \times N)$ array of nonlinear equations. If we then compute partial derivatives of each equation by each unknown in the order $u_1{}^1, u_2{}^1, \ldots, u_N{}^1, u_1{}^2, \ldots, u_N{}^2, \ldots, u_1{}^M, \ldots, u_N{}^M, v_1{}^1, \ldots, v_N{}^M, w_1{}^1, \ldots, w_N{}^M, F_1{}^1, \ldots, F_N{}^M$, then we get

$$\begin{bmatrix} A_{11} & A_{12} & A_{13} & 0 \\ A_{21} & A_{22} & A_{23} & 0 \\ A_{31} & A_{32} & A_{33} & A_{34} \\ 0 & 0 & A_{43} & A_{44} \end{bmatrix}\begin{bmatrix} \Delta\mathbf{u} \\ \Delta\mathbf{v} \\ \Delta\mathbf{w} \\ \Delta\mathbf{F} \end{bmatrix} = \begin{bmatrix} A_{15} \\ A_{25} \\ A_{35} \\ 0 \end{bmatrix} \quad \text{(A7)}$$

where the form of the matrix elements A_{ij} will depend on the boundary conditions.‡

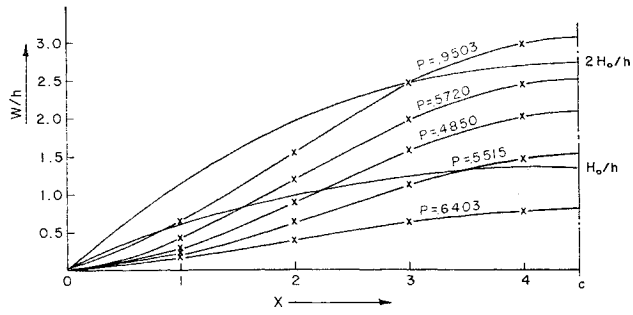

Fig. 10 Deflection modes compared with initial rise parabola of shell and reversed parabola ($\lambda = 3$ fixed edges, 8×8 grid).

A-3. Modifications for Adding $\tilde{q}$ as Unknown

For some problems it is convenient to regard $\tilde{q}$ as a variable and specify another quantity as an independent variable. For example, if we define

$$w_{AV} = \frac{1}{MN}\sum_{i=1}^{N}\sum_{j=1}^{M} w_i^j \quad \text{(A8)}$$

then if $\tilde{q}$ is included as the $MN + 1$st member of a modified $\mathbf{w}^*$ vector, then the A_{33} must be modified with an $MN + 1$st row with entries 1 and column with entries 1 (or suitable multiples of these for nonuniform loading). Also (A8) goes on the right side in the $3MN + 1$st entry as

$$MN \cdot w_{AV} = \sum_{i=1}^{N}\sum_{j=1}^{M} w_i^j$$

References

[1] Volmir, A. S., "A Translation of Flexible Plates and Shells," TR AFFDL-TR-66-216, April 1967, Air Force Flight Dynamics Lab.

[2] Huang, N. C., "Unsymmetrical Buckling of Thin Shallow Spherical Shells," *Journal of Applied Mechanics*, Vol. 31, 1964, pp. 447–457.

[3] Bushnell, D., "Bifurcation Phenomena in Spherical Shells under Concentrated and Ring Loads," *AIAA Journal*, Vol. 5, No. 11, Nov. 1967, pp. 2034–2040.

[4] Archer, R. R. and Lange, C. G., "Nonlinear Dynamic Behavior of Shallow Spherical Shells," *AIAA Journal*, Vol. 3, No. 12, Dec. 1965, pp. 2312–2317.

[5] Hildebrand, F. B., *Introduction to Numerical Analysis*, McGraw-Hill, New York, 1956, pp. 450–451.

[6] Weinitschke, H., "On the Stability Problem for Shallow Spherical Shells," *Journal of Mathematics and Physics*, Vol. XXXVIII, No. 4, Jan. 1960, p. 230.

[7] Archer, R. R. and Hsueh, P. K., "On the Large Deflection of Shallow Rectangular Shell Panels," TR-EM68-3, Aug. 1968, Engineering Research Institute, Univ. of Massachusetts, Amherst.

‡ Explicit expressions for the A_{ij} are too lengthy to record here; see Ref. 7.